

INITIAL DATA FROM AN ELECTRON CLOUD DETECTOR IN A QUADRUPOLE MAGNET AT CESR^{TA}*

J. P. Sikora[†], S. Barrett, M. G. Billing, J. A. Crittenden, K. A. Jones, Y. Li, T. O'Connell
CLASSE, Cornell University, Ithaca, NY 14853, USA

Abstract

In September 2016, we installed a detector in a quadrupole magnet that measures electron cloud density using two independent techniques. Stripline electrodes collect cloud electrons which pass through holes in the beam-pipe wall. The array of small holes helps to shield the striplines from the beam-induced electromagnetic pulse. The beam-pipe chamber has also been designed so that microwave measurements of the electron cloud density can be performed. The resonant microwaves are confined to be within the 56 cm length of the quadrupole. The detector is placed in a newly installed quadrupole that is adjacent to an existing lattice quadrupole of the same polarity. Since they are powered independently, their relative strengths can be varied with stored beam – allowing electron cloud measurements to be made as a function of gradient. This paper presents the first data obtained with this detector with trains of positron bunches at 5.3 GeV. The detector is installed in the Cornell Electron Storage Ring and is part of the test accelerator program for the study of electron cloud build-up using electron and positron beams from 2 to 5 GeV.

INTRODUCTION

At the Cornell Electron Storage Ring (CESR), comparisons have been made between electron cloud (EC) simulations and density measurements for several years. This work has been carried out both with and without external magnetic fields as part of the CESR^{TA} test accelerator program [1, 2].

In September 2016, a detector was installed in a quadrupole magnet that uses two independent techniques to measure EC density. One technique is comprised of a stripline electrode that is partially shielded from the electromagnetic pulse of the beam by an array of small holes in the beam-pipe wall. Cloud electrons pass through the holes, are collected on the stripline electrode and the voltage digitized by an oscilloscope [3–5]. We used a similar detector to observe trapping of the electron cloud in a quadrupole [6]. The second technique is to resonantly excite the beam-pipe in a TE_{11} mode using one beam position monitor (BPM) button, and a second button to pick up the resonant response and display it on a spectrum analyzer. A train of bunches in the storage ring generates a periodic EC density that modulates the resonant frequency of the beam-pipe at the beam repetition frequency of 390 kHz. This produces phase mod-

ulation sidebands in the received spectrum. The chamber for this detector was designed to employ this technique [5]. Figure 1 shows the location of the detectors on the chamber. There is a single stripline azimuthally centered on the pole face of the quadrupole, and a pair of striplines offset from the center of the pole face. BPM buttons are located on the bottom and on the radial inside of the chamber, allowing either horizontal or vertical TE_{11} modes to be excited.

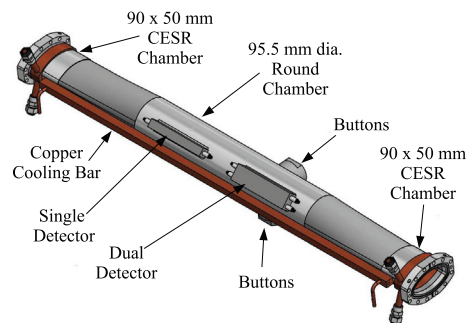


Figure 1: The detector chamber showing the location of the single and dual stripline detectors as well as the buttons that are used for microwave measurements.

DETECTOR CONFIGURATION

For the microwave measurements, only the horizontally oriented buttons have been used so far. The output of a signal generator is amplified to 5 W and is routed to one of the buttons. A circulator and bandpass filter are used to reduce the direct beam signal from the button back to the amplifier. The signal from the second button is routed to the spectrum analyzer through a bandpass filter and 10 dB attenuator. The drive frequencies are chosen to be near the center of the TE_{11} resonances, but may be slightly offset to avoid coincidence with 390 kHz beam revolution-frequency harmonics.

The stripline is biased at 50 V in order to retain any secondary electrons produced on its surface by the incoming cloud electrons. It is capacitively coupled to the signal cable, with bias being applied through a 10 k Ω resistor along with a 1 M Ω resistor to ground as shown in Fig. 2. One end of the stripline is terminated in 50 Ω , the other is routed to the oscilloscope through a 50 Ω cable, a pair of 1.2 GHz low-pass filters and a pair of +20 dB amplifiers. The detector biasing and termination arrangement was checked with a time delay reflectometer that showed a reasonably good match through the biasing network and stripline to the 50 Ω termination.

* This work is supported by the US National Science Foundation PHY-0734867, PHY-1002467 and the US Department of Energy DE-FC02-08ER41538, DE-SC0006505.

[†] jps13@cornell.edu

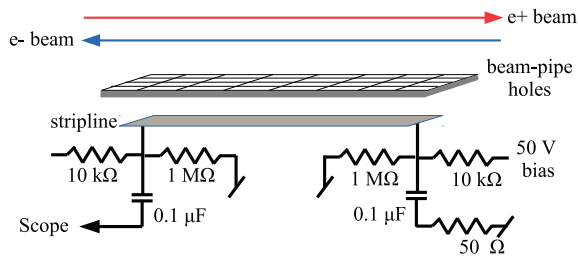


Figure 2: Stripline configuration with its connections to bias, ground and a digitizing oscilloscope.

MEASUREMENTS

A 20-bunch train of 5.3 GeV positrons was injected into the storage ring with a bunch spacing of 14 ns. With a beam current of 160 mA, the bunch population is 1.28×10^{11} particles/bunch. As the field of the quadrupole with the detectors is changed, the field of an adjacent quadrupole is adjusted to compensate and maintain stored beam. At various quadrupole fields and uniform bunch currents, data was taken with both the microwave and stripline detectors.

Microwave Measurements

Microwave data was taken using the two lowest horizontal TE_{11} modes. The spatial extent of these modes is illustrated in Fig. 3, where a simulation of the electric field squared (E^2) is superposed on the quad and chamber geometry. The sensitivity of the microwave measurement is proportional to the integral of the product of E^2 and the local EC density [7]. As shown in the figure, this sensitivity is mostly confined to the length of the quadrupole.

The EC density is calculated from the spectrum of the beam-pipe response, using the ratio of the phase modulation sideband amplitudes to the amplitude at the drive frequency [7]. An example of a such a spectrum is given in Fig. 6. An approximation used in this calculation is that the EC density quickly comes to a fixed value at the beginning of a bunch train and falls quickly to zero at the end of the train. This approximation has given results close to those obtained when using a full simulation of the EC density time profile [8]. The present calculation also neglects the influence of the magnetic field on the microwave-induced motion of the electrons, which will affect the calibration of the measurement.

Plots of the peak EC density versus beam current at four quadrupole field settings are given in Figs. 4 and 5. The EC density measured by mode 1 (Fig. 4) at a given quadrupole field has a fairly linear dependence on beam current, and the EC density generally decreases with increasing magnetic field. For mode 2 the result is similar, but there is a saturation in the measured EC density with increased quadrupole field. As shown in in Fig. 5, at 3.5 T/m the EC density measurement actually decreases above about 150 mA.

The phase modulation sideband amplitude used in calculating the EC density is the average of the upper (USB) and lower (LSB) 390 kHz sidebands. In examining the received

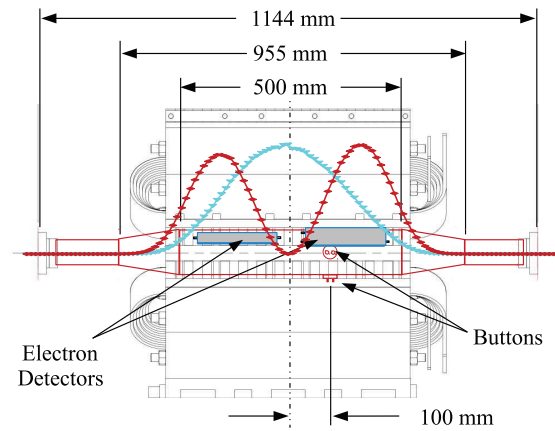


Figure 3: The quadrupole and beam-pipe with a plot the E^2 value of the $m = 1$ and $m = 2$ horizontal TE_{11} modes.

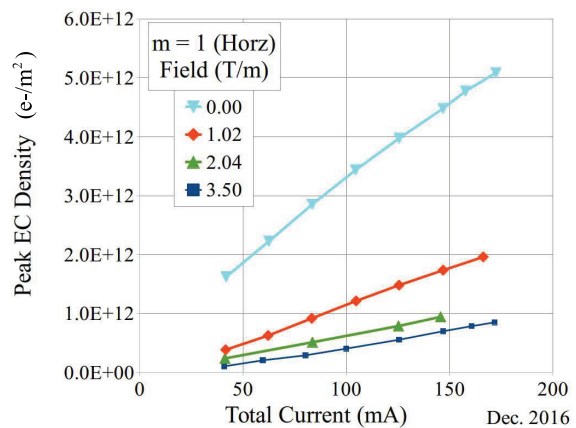


Figure 4: Measured EC density versus total current with a 20-bunch train of positrons at 5.3 GeV using the $m = 1$ mode.

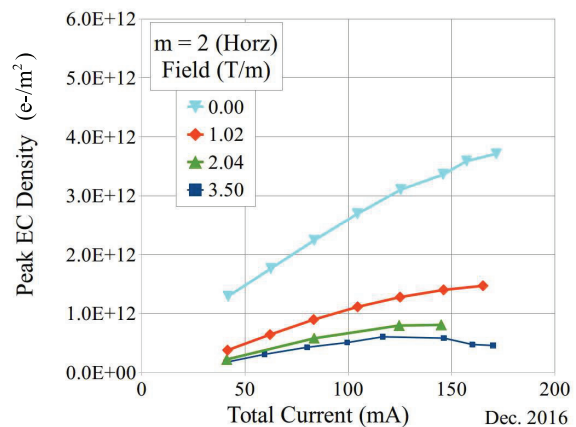


Figure 5: Measured EC density versus total current with a 20-bunch train of positrons at 5.3 GeV using the $m = 2$ mode.

spectra as shown in Fig. 6, it is found that as the beam current increases above 100 mA (with the quadrupole field at 3.5 T/m), the amplitude of the LSB continues to increase

but the USB amplitude decreases significantly. The drive signal also contains a 0.001 radian phase modulation reference at 410 kHz. The reference sidebands at ± 410 kHz are seen near the ± 390 kHz phase modulation sidebands produced by the electron cloud. The amplitudes of the 410 kHz reference sidebands do not change over the course of the measurement, so a resonant frequency shift (due to heating of the chamber for example) seems to be ruled out. It can also be seen that the beam was longitudinally unstable at higher currents.

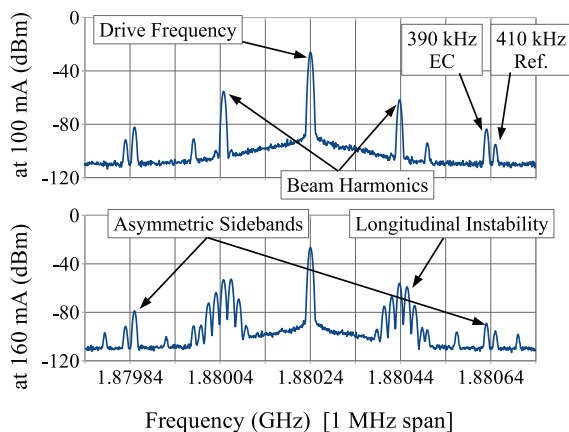


Figure 6: Response of the detector chamber at 100 mA and 160 mA beam current with the quadrupole field at 3.5 T/m. At 160 mA, the 390 kHz sidebands are asymmetric.

Stripline Measurements

With a 20-bunch train of positrons and various settings of the quadrupole field, the signals from the stripline detectors were recorded on an oscilloscope. The electron cloud signal is not easily seen, especially in the presence of direct beam signal, which is larger than expected. Figure 7 shows data from the stripline centered on the quadrupole face with a total beam current of 160 mA. The plot is the difference between data taken with the stripline biased at 50 V and at 0 V. So the plot should be dominated by the signal due to the electron cloud. With the quadrupole at a nominal 0 T/m, an electron signal is clearly visible. But at 3.5 T/m, the signal is more difficult to see.

SUMMARY AND CONCLUSIONS

Microwave measurements show a roughly linear dependence of the peak electron cloud density with beam current for all measured values of quadrupole field. As the quadrupole field is increased from zero to 3.5 T/m, the measured EC density decreases by about a factor of five. However, there is a saturation in the data for the $m = 2$ mode that has not been explained. The effect of the magnetic field on the sensitivity of the measurement has not been taken into account. This is an important next step in the analysis.

The signal from the stripline detector is small even at the highest beam current, but is consistent with the microwave data in that it decreases significantly with quadrupole field.

ISBN 978-3-95450-182-3

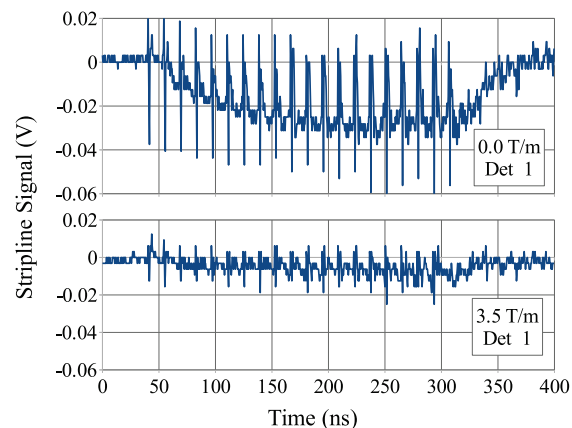


Figure 7: Stripline data with a 160 mA 20-bunch train of positrons at quadrupole fields of 0 and 3.5 T/m, plotting the difference between the bias 50 V and 0 V signals.

REFERENCES

- [1] M.G. Billing *et al.*, “The Conversion of CESR to Operate as the Test Accelerator, CestrTA. Part 3: electron cloud diagnostics,” *Journal of Instrumentation* **11** P04025 (2016), doi:10.1088/1748-0221/11/04/P04025.
- [2] J. P. Sikora *et al.*, “Cross-Calibration of Three Electron Cloud Density Detectors at CESR-TA,” in Proc. of IBIC’14, Monterey, California, USA, Sept. 2014, THCB1, pp. 722-26, (2014).
- [3] J.A. Crittenden *et al.*, “Shielded Button Electrodes for Time-Resolved Measurements of Electron Cloud Buildup,” *Nucl. Instrum. Methods Phys. Res.*, **A749**, pp. 42-46, (2014), <http://dx.doi.org/10.1016/j.nima.2014.02.047>, Preprint, arXiv:1311.7103 [physics.acc-ph].
- [4] J.A. Crittenden *et al.*, “Progress in Detector Design and Installation for Measurements of Electron Cloud Trapping in Quadrupole Magnetic Fields at CestrTA,” in Proc. of IPAC’16, Busan, Korea, May 2016, WEPW004, p. 2420, (2016).
- [5] J.P. Sikora *et al.*, “Design of an Electron Cloud Detector in a Quadrupole Magnet at CestrTA,” in Proc. of IBIC’16, Barcelona, Spain, Sept. 2016, WEPG35, pp. 705–708, 2017.
- [6] M. G. Billing *et al.*, “Measurement of Electron Trapping in the Cornell Electron Storage Ring,” *Phys. Rev. ST Accel. Beams* **18**, 041001 (Apr. 2015).
- [7] J.P. Sikora *et al.*, “Electron Cloud Density Measurements in Accelerator Beam-Pipe Using Resonant Microwave Excitation,” *Nucl. Instrum. Methods Phys. Res.*, **A754**, pp. 28-35 (2014), <http://dx.doi.org/10.1016/j.nima.2014.03.063>, Preprint, arXiv:1311.5633 [physics.acc-ph].
- [8] J.P. Sikora, *et al.*, “Resonant TE Wave Measurement of Electron Cloud Density Using Multiple Sidebands,” in Proc. of IBIC’13, Oxford, United Kingdom, September 2013, TUPF34, (2013).